

Contribution of Xanthine Oxidoreductase to Mammary Epithelial and Breast Cancer Cell Differentiation In Part Modulates Inhibitor of Differentiation-1

Mehdi A. Fini^{1,2,4}, Jenifer Monks^{1,2}, Susan M. Farabaugh³, and Richard M. Wright^{1,2}

Abstract

Loss of xanthine oxidoreductase (XOR) has been linked to aggressive breast cancer *in vivo* and to breast cancer cell aggressiveness *in vitro*. In the present study, we hypothesized that the contribution of XOR to the development of the normal mammary gland may underlie its capacity to modulate breast cancer. We contrasted *in vitro* and *in vivo* developmental systems by differentiation marker and microarray analyses. Human breast cancer microarray was used for clinical outcome studies. The role of XOR in differentiation and proliferation was examined in human breast cancer cells and in a mouse xenograft model. Our data show that XOR was required for functional differentiation of mammary epithelial cells both *in vitro* and *in vivo*. Poor XOR expression was observed in a mouse ErbB2 breast cancer model, and pharmacologic inhibition of XOR increased breast cancer tumor burden in mouse xenograft. mRNA microarray analysis of human breast cancer revealed that low XOR expression was significantly associated with time to tumor relapse. The opposing expression of XOR and inhibitor of differentiation-1 (Id1) during HC11 differentiation and mammary gland development suggested a potential functional relationship. While overexpression of Id1 inhibited HC11 differentiation and XOR expression, XOR itself modulated expression of Id1 in differentiating HC11 cells. Overexpression of XOR both inhibited Id1-induced proliferation and -stimulated differentiation of Heregulin- β 1-treated human breast cancer cells. These results show that XOR is an important functional component of differentiation whose diminished expression contributes to breast cancer aggressiveness, and they support XOR as both a breast cancer biomarker and a target for pharmacologic activation in therapeutic management of aggressive breast cancer. *Mol Cancer Res*; 9(9); 1242–54. ©2011 AACR.

Introduction

Xanthine oxidoreductase (XOR) seems to exert an important but poorly defined role in modulating the pathogenesis of breast cancer. Loss of XOR activity has been linked to aggressive breast cancer (1), and both in mouse models of mammary carcinogenesis and in human breast cancer patients, decreasing epithelial XOR was associated with and/or predictive of poor clinical outcome and the degree of breast cancer aggressiveness (1–4). Patients without evident epithelial XOR expression had the most aggressive breast cancer and had 2.5-fold increased risk of recurrence

compared with patients expressing normal or modestly reduced XOR (1).

Consistent with these clinical observations, we observed that XOR expression was markedly reduced in highly invasive mammary tumor cells in culture compared with expression in normal mouse and human epithelial cells (5). The contribution of XOR to tumor cell aggressiveness *in vitro* was investigated using the basal breast cancer cell line MDA-MB-231 and the luminal breast cancer cell line MCF-7. We observed that overexpression of an XOR cDNA in MDA-MB-231 cells, possessing both weak XOR expression and high migratory capacity, inhibited migration and expression of genes that mediate breast cancer invasiveness including COX-2, matrix metalloproteinase (MMP)-1, and MMP-3 *in vitro*. Conversely, pharmacologic inhibition of XOR in MCF-7 cells possessing both intermediate XOR expression and weak migratory capacity increased COX-2 expression and stimulated migration *in vitro* (5).

A mechanism by which XOR could suppress breast cancer aggressiveness was suggested by its involvement in lactation. Although it is poorly expressed in virgin mammary glands (6), XOR is an abundant milk protein that is highly expressed in mammary tissue during pregnancy and lactation (7–9) where it plays an important functional role

Authors' Affiliations: ¹Webb-Waring Center, Department of Medicine, ²Division of Pulmonary and Critical Care Medicine, ³Division of Obstetrics & Gynecology, and ⁴Cardiovascular Pulmonary Research Laboratory, The University of Colorado Denver, Anschutz Medical Campus, Aurora, Colorado

Corresponding Authors: Richard M. Wright, Department of Medicine, University of Colorado Denver, Campus Box C-322, 12850 East Montview Boulevard, Aurora, CO 80045. Phone: 303-724-4780; Fax: 303-724-4779; E-mail: Richard.m.Wright@ucdenver.edu or Mehdi A. Fini, Department of Medicine, University of Colorado Denver, Campus Box C-321, 12850 East Montview Boulevard, Aurora, CO 80045. Phone: 303-724-4781; Fax: 303-724-4779; E-mail: Mehdi.Fini@ucdenver.edu

doi: 10.1158/1541-7786.MCR-11-0176

©2011 American Association for Cancer Research.

in the development of the lactating mammary gland and in cultured HC11 cells (6, 7, 9–13). XOR is induced in mammary gland epithelial cells late in pregnancy, further stimulated by lactation, and then precipitously lost during involution (6, 10, 11). In cultured HC11 cells, XOR can be induced by the lactogenic hormones cortisol (or dexamethasone), insulin, and prolactin (6, 10). The importance of XOR to lactation was corroborated by knockout genetics in mice. Although homozygous XOR knockout mice (XOR^{-/-}) showed early neonatal lethality, heterozygous XOR knockout mice (XOR^{+/-}) exhibited disrupted formation of the milk fat globule (MFG; ref. 14). Recent data showed that XOR forms a sulphhydryl bond-dependent complex with butyrophilin and adipophilin in the MFG membrane. This physical interaction between XOR, butyrophilin, and adipophilin seems to be essential for the formation of the MFG during lactation (9, 12).

XOR is a member of the molybdoflavoproteins that catalyzes the formation of uric acid from xanthine and hypoxanthine. During purine oxidation, XOR is a source of reactive oxygen species, reactive nitrogen species, and uric acid that could potentially regulate many aspects of epithelial cell function or signaling that are involved in breast cancer pathogenesis, including regulation of COX-2 (5, 15, 16), MMP-1 (17), or other factors that contribute to tumor promotion or metastasis (18).

Data shown in the present investigation support the hypothesis that the contribution of XOR to development *in vitro* and *in vivo* (12, 14) mediates the suppressive effect of XOR on breast cancer.

Materials and Methods

Reagents

Most reagents, buffers, substrates, PAGE supplies, epidermal growth factor (EGF), insulin, and Heregulin- β 1 (HRG β 1) were purchased from Sigma-Aldrich. Media for cell culture were obtained from Gibco/BRL. FBS was from Gemini Bioproducts. The following primary antibodies were used: rabbit anti- β -actin (A-2066) from Sigma; rabbit antibody to XOR (100-4183) from Rockland, Inc.; mouse and human reactive goat anti- β -casein (sc-17969), antibodies to inhibitor of differentiation (Id) proteins 1 (sc-488), 2 (sc-489), 3 (sc-490), and 4 (sc-491) were all from Santa Cruz Biotechnology, Inc. The following antibodies were used for fluorescent labeling: FITC-conjugated donkey anti-Rat IgG (712-095-150; Jackson ImmunoResearch) and FITC-conjugated donkey anti-mouse IgG (715-095-150; Jackson ImmunoResearch). The following horseradish peroxidase-conjugated secondary antibodies were also purchased from Santa Cruz Biotechnology, Inc.: goat anti-rat IgG (sc-2006), goat anti-mouse IgG (sc-2005), and goat anti-rabbit IgG (sc-2004). Antibody used for the detection of XOR was previously described (12).

Cell culture, proliferation, and viability

Mouse and human cells were grown as previously described (5). MCF-7 and MDA-MB-231 human cancer

cells were obtained from the American Type Culture Collection (HTB-22 and HTB-26). Cell number and viability were determined by sulforhodamine-B (SRB) assay. Cells were plated in triplicate (10,000 cells per well) on 48-well transparent, flat-bottomed tissue culture plates. After the indicated treatments, cells were fixed in 10% trichloroacetic acid overnight. A solution of 0.4% SRB was added to each well, and plates were washed after 30 minutes of incubation at room temperature. SRB dye was solubilized on the plates in 10 mmol/L Tris, pH 7.5, and dye was quantitated on a TECAN Infinite M200 plate reader (TECAN) at an absorbance of 465 nm. Data were calculated as 465 nm absorbance minus background absorbance obtained at 690 nm, and figures show the mean \pm SD of at least 3 replicates.

Oil Red O staining and quantitation

Cells were cultured in 12-well trays on sterile glass slides, and after the indicated treatments, slides were washed with PBS, fixed with 3.7% formaldehyde at room temperature, and washed again with PBS. Slides were then stained with 0.5% Oil Red O solution prepared in isopropanol. Slides were then rinsed with water, counterstained with hematoxylin, and treated with Crystal/Mount mounting media for preservation and photography. Oil Red O staining was quantitated by solubilizing the stain in each well with 2 mL of anhydrous isopropanol and determining absorbance at 550 nm with a TECAN Infinite M200 plate reader. All figures show the mean \pm SD of at least 3 replicates.

SDS-PAGE and Western immunoblot analysis

Western immunoblots were run as previously described (13). Corroboration of the Id1 protein detected at 17 kDa using the Santa Cruz antibody sc-488 was established using lysates of MCF-7 cells that had been transfected with pCMV6-Id1, which expresses the mature Id1 protein as described below. This clearly distinguished Id1 from higher molecular weight cross-reactive material obtained with sc-488 antibody (19), and all gels shown here display the confirmed 17-kDa Id1 antigen. Antigen-antibody complexes were detected by reaction with an ECL Western blotting detection kit according to manufacturer's instruction (Amersham Life Sciences). Each experiment was run in duplicate or triplicate, and representative immunoblots are shown.

Thioglycolate-elicited macrophages

Verification of the antibody used for XOR immunofluorescence analysis was obtained by generating thioglycolate-elicited macrophages from XOR^{+/+} and XOR conditional knockout strains (manuscript in preparation). Briefly, Cre-LoxP technology was used to knockout XOR specifically in myeloid lineage cells in C57Bl/6 mice. LoxP-inserted XOR strains were bred to homozygosity for LoxP sites flanking critical exons in the XOR gene, generating XOR^{fl/fl} mice. These mice were bred to mice expressing the Cre recombinase under the control of the

myeloid-specific gene promoter for LysM. The resulting progeny XOR^{fl/fl}/LysM-Cre was treated with thioglycolate by intraperitoneal injection, and 3 days later, leukocytes were harvested by peritoneal lavage. Western blots were run using 50 µg of whole-cell extract.

Transfection and generation of stable cell lines

Several stably transfected cell lines were generated from wild-type MCF-7 cells for this study. Prior to transfection, MCF-7 cells were genotyped at the University of Colorado Denver (UCD) DNA Sequence Core to verify lineage. MCF-7-Myc and MCF-7-Myc-XOR were generated as previously described using G418 selection (5). MCF-7 cells were transfected with pCMV-Myc empty vector or with the XOR cDNA expression vector pCMV-Myc-XOR-1 in cotransfection reactions with pCI-NEO at a 1:0.1 mass ratio as described (5). This generated the cell lines MCF-7-Myc and MCF-7-Myc-XOR. HC11-pCMV6-Id1 and MCF-7-pCMV6-Id1 were generated by cotransfection of wild-type HC11 and MCF-7 with the Id1 expression vector pCMV6-Id1 (sc-125462) and pCI-NEO. Id1 cDNA cloned into the pCMV6 expression vector was obtained from OriGene Technologies Inc. and verified by restriction endonuclease cleavage analysis and Western immunoblot. Stable transfectants of all cell lines were selected with G418 present at 600 µg/mL in rich growth medium and maintained at 200 µg/mL G418. All stable cell lines used in the present investigation were derived from pools of at least 300 single colonies.

Anti-XOR-siRNA

siRNA against mouse XOR was obtained from Dharmacon Inc. Initially, we tested the Dharmacon On-Target-Plus-Smartpool for inhibition of XOR activity in HC11 cells. This pool consisted of 4 optimized siRNA duplexes. Knockdown of HC11 XOR activity was 95% in cells assayed 3 days after transfection. We used the On-Target-Plus-sicontrol (D-001810-10-05) as a scrambled siRNA control that possessed no sequence homology with the mouse genome. Individual anti-XOR-siRNAs from the original Smart Pool were then tested for XOR activity silencing. Transfection of siRNA duplex-9 reduced XOR activity from 125 pmol U.A./min/mg in the scrambled control to 7.5 pmol U.A./min/mg, approximately 94% knockdown of XOR activity. The anti-XOR-siRNA duplex-9 has the following sequence: sense strand 5'-CCAUAAGAAUCUCCGUACAUU-3' and antisense strand 5'-PUGUACGGAGAUUCUUAUGGUU-3' corresponding to nucleotides 3,573 through 3,591 of the mouse mRNA sequence (20). Anti-mouse-XOR-siRNA duplex-9 was routinely transfected at a concentration of 100 nmol/L with the DharmaFECT-1 (T-200-01-07-01) transfecting reagent as recommended by the supplier.

Histologic and immunofluorescence analyses of mammary tissue

Paraffin-embedded tissue sections were prepared from C57Bl/6 mouse mammary glands harvested at day 7 of

pregnancy (P7) and lactation day 1 (L1). Sections were deparaffinized, rehydrated, and antigen retrieval was conducted with Vector Antigen Unmasking Solution (H-3300; Vector Laboratories). Slides were allowed to cool and were then permeabilized with 0.2% Triton X-100 for 5 minutes and blocked with 10% donkey serum in PBS. Primary antibody solutions were as follows: 1:100 rabbit anti-XOR (ab6194; Abcam) and rabbit anti-Id1 (sc-488; Santa Cruz). The immunostain was visualized with a donkey anti-rabbit IgG conjugated to DyLight 549 (711-506-152; Jackson ImmunoResearch). Sections were costained with wheat germ agglutinin (AlexaFluor 488 conjugate, W11261; Invitrogen) to show tissue morphology. Slides were mounted with Prolong Gold + DAPI (P36935; Invitrogen), and images were captured in the CU Denver, Anschutz Medical Center Light Microscopy Core Facility, using the Olympus IX81 inverted microscope, 100 watt Hg lamp, and Hamamatsu ORCA IIER CCD camera, using Slidebook Acquisition Software (Intelligent Imaging Innovations, Inc.).

Tumor xenograft and animal treatment

MDA-MB-231 cells were verified by DNA profiling at the University of Colorado Cancer Center DNA Sequencing & Analysis Core. Cells were grown as described previously, harvested from subconfluent cultures, and resuspended in 50% growth factor-reduced Matrigel (354230; BD Biosciences). Cells were tested for mycoplasma by using the MycoAlert Assay (LT07-218; Lonza) prior to injection into 6-week-old athymic nude (*nu/nu*) mice, purchased from the National Cancer Institute, orthotopically under the nipple of the inguinal mammary gland on one side (21, 22). Mice were given allopurinol (25 mg/kg/d), oxypurinol (25 mg/kg/d), or Y-700 (5 mg/kg/d) in drinking water (23, 24), refreshed twice per week. Current standard technique involves an external caliper for the determination of volume of subcutaneously xenografted tumors *in vivo* in which tumor volume is calculated by the use of the modified ellipsoid formula: $1/2(\text{length} \times \text{width}^2)$, or $(v = xy^2)$, as described (25). Tumors were allowed to grow for 12 weeks, mice were euthanized with CO₂ and cervical dislocation, and tumors were harvested for analysis. Mice were housed 4 per cage, fed *ad libitum*, with a 12-hour light-dark cycle, in the UCD, Anschutz Medical Campus Animal Care Facility. All procedures were approved by the Institutional Animal Care and Use Committee.

mRNA microarray data mining

Expression of XOR mRNA during mouse mammary gland development was analyzed using publicly shared microarray databases (26, 27). Data were normalized and displayed using Genespring GX 7.3.1 software (Agilent Technologies). Normalized mRNA expression for XOR and Id genes was obtained over the entire developmental time course comprising: (i) virgin weeks, 6, 10, and 12; (ii) pregnancy days, 1, 3, 8.5, 14.5, 17, and 19; (iii) lactation days, 1, 2, 3, 7, and 9; and (4) forced-weaning involution at days 1, 2, 3, 4, and 20.

XOR gene expression and clinical outcome data in human breast cancer were obtained from the publicly available Wang

data set, which comprises 286 lymph node–negative breast cancer patients (28). All tumor samples were mean centered for XOR expression and divided into 2 groups: samples that express the gene above or below the mean (high XOR or low XOR, respectively). Kaplan–Meier survival curves were generated using WinStat for Excel (R. Fitch Software) where *P* values denote log-rank analysis. Normalization was obtained from the National Center for Biotechnology Information Gene Expression Omnibus Web site (GSE2034).

Results

XOR mRNA and protein expression were closely linked to the differentiated state of the mammary gland *in vivo*

Expression of XOR throughout mouse mammary gland development *in vivo* was analyzed by mRNA microarray

data mining. We observed an initial spike in XOR mRNA expression just before the onset of pregnancy that was followed by decline until midway through pregnancy. XOR expression then increased during the early stages of secretory differentiation during pregnancy, but after the principal proliferative phase associated with ductal elongation and branching, it peaked at full secretory activation of lactation and then declined again during mammary gland involution. Thus, XOR mRNA expression was closely linked to the differentiation of the mammary gland associated with lactation (Fig. 1A). Consistent with these observations, XOR protein antigen was nearly undetectable early in pregnancy but was highly expressed during lactation wherein it was associated with the lactating MFG (Fig. 1B). The validity of the antibody used for XOR immunofluorescence analysis was established by Western immunoblot

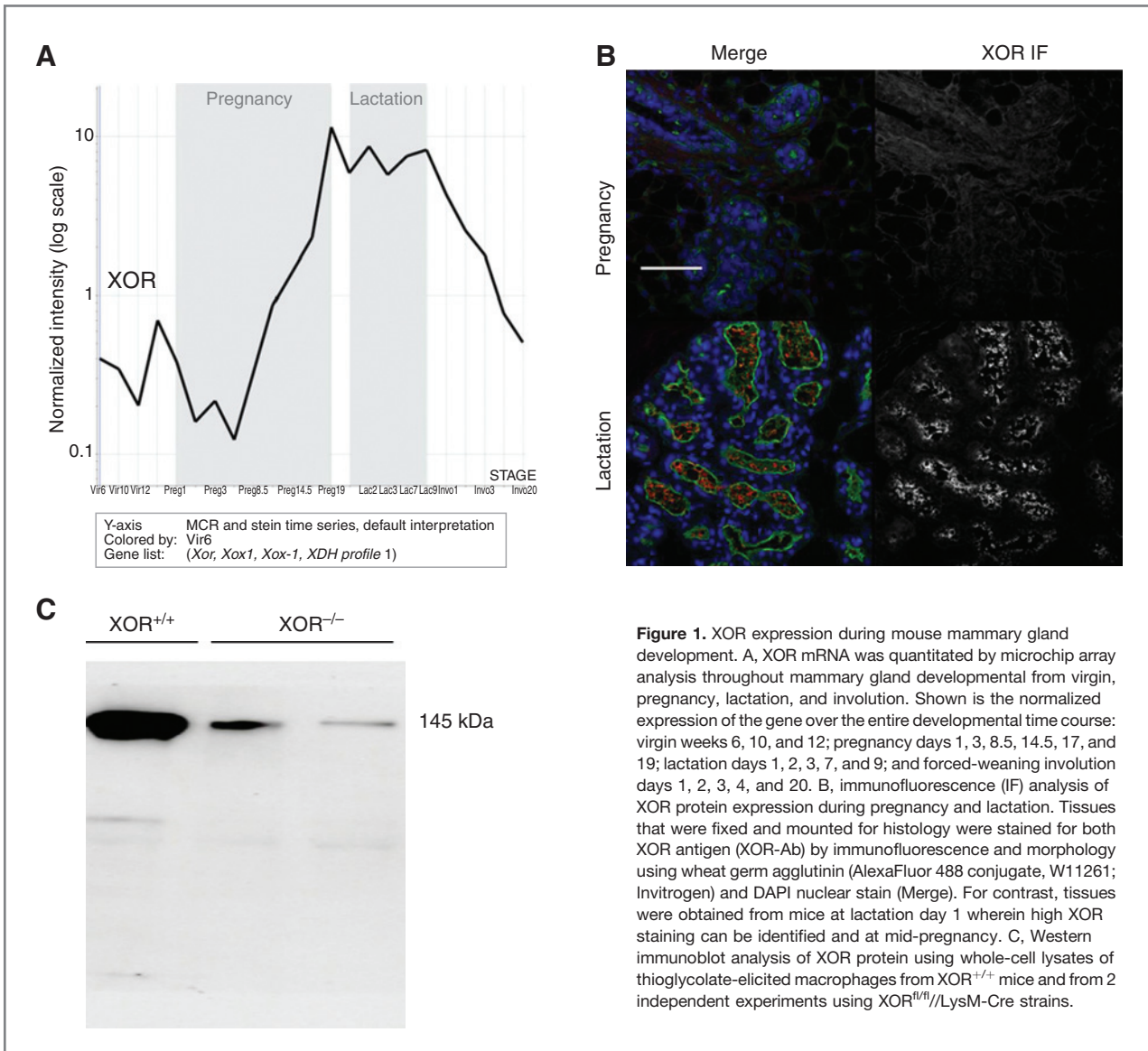


Figure 1. XOR expression during mouse mammary gland development. A, XOR mRNA was quantitated by microchip array analysis throughout mammary gland developmental from virgin, pregnancy, lactation, and involution. Shown is the normalized expression of the gene over the entire developmental time course: virgin weeks 6, 10, and 12; pregnancy days 1, 3, 8.5, 14.5, 17, and 19; lactation days 1, 2, 3, 7, and 9; and forced-weaning involution days 1, 2, 3, 4, and 20. B, immunofluorescence (IF) analysis of XOR protein expression during pregnancy and lactation. Tissues that were fixed and mounted for histology were stained for both XOR antigen (XOR-Ab) by immunofluorescence and morphology using wheat germ agglutinin (AlexaFluor 488 conjugate, W11261; Invitrogen) and DAPI nuclear stain (Merge). For contrast, tissues were obtained from mice at lactation day 1 wherein high XOR staining can be identified and at mid-pregnancy. C, Western immunoblot analysis of XOR protein using whole-cell lysates of thioglycolate-elicited macrophages from XOR^{+/+} mice and from 2 independent experiments using XOR^{fl/fl}/LysM-Cre strains.

Downloaded from <http://aacrjournals.org/mcr/article-pdf/9/9/1242/3148004/1242.pdf> by guest on 22 April 2025

analysis of whole-cell extracts derived from thioglycolate-elicited macrophages from XOR^{+/+} and XOR^{-/-} mice using a XOR^{fl/fl}/LysM-Cre mouse strain (Fig. 1C).

XOR activity, β -casein, and neutral lipids were coordinately induced by differentiation of HC11 cells *in vitro*

Differentiation of HC11 cells with lactogenic hormones was achieved in several distinct steps (29). Cells were grown in rich culture medium in the presence of EGF and insulin. After reaching confluency, they were shifted into starvation medium consisting of serum-free growth medium supplemented with insulin but not EGF (29), and after 48 hours of starvation, they were shifted into DIP medium consisting of serum-free growth medium supplemented with dexamethasone, insulin, and prolactin. Cells were commonly assayed 1, 2, or 3 days following the shift into DIP medium

(Fig. 2A). We observed that oxypurinol-inhibitable XOR activity (Fig. 2B), β -casein (Fig. 2C), and vesicle neutral lipids (Fig. 2D) were coordinately induced by *in vitro* differentiation of HC11 cells.

Inhibition of XOR blocked expression of β -casein protein and neutral lipid in differentiating HC11 cells

To determine whether XOR activity was required for differentiation, HC11 cells were differentiated *in vitro* in the presence of 3 different pharmacologic inhibitors of XOR: allopurinol, oxypurinol, or Y-700. Inhibitors applied immediately before the shift into DIP medium blocked β -casein accumulation compared with the uninhibited control (Fig. 3A). Allopurinol seemed to be slightly less efficient than oxypurinol or Y-700. To corroborate the effect of pharmacologic inhibitors, we transfected HC11 cells immediately before the shift into DIP medium with either siRNA

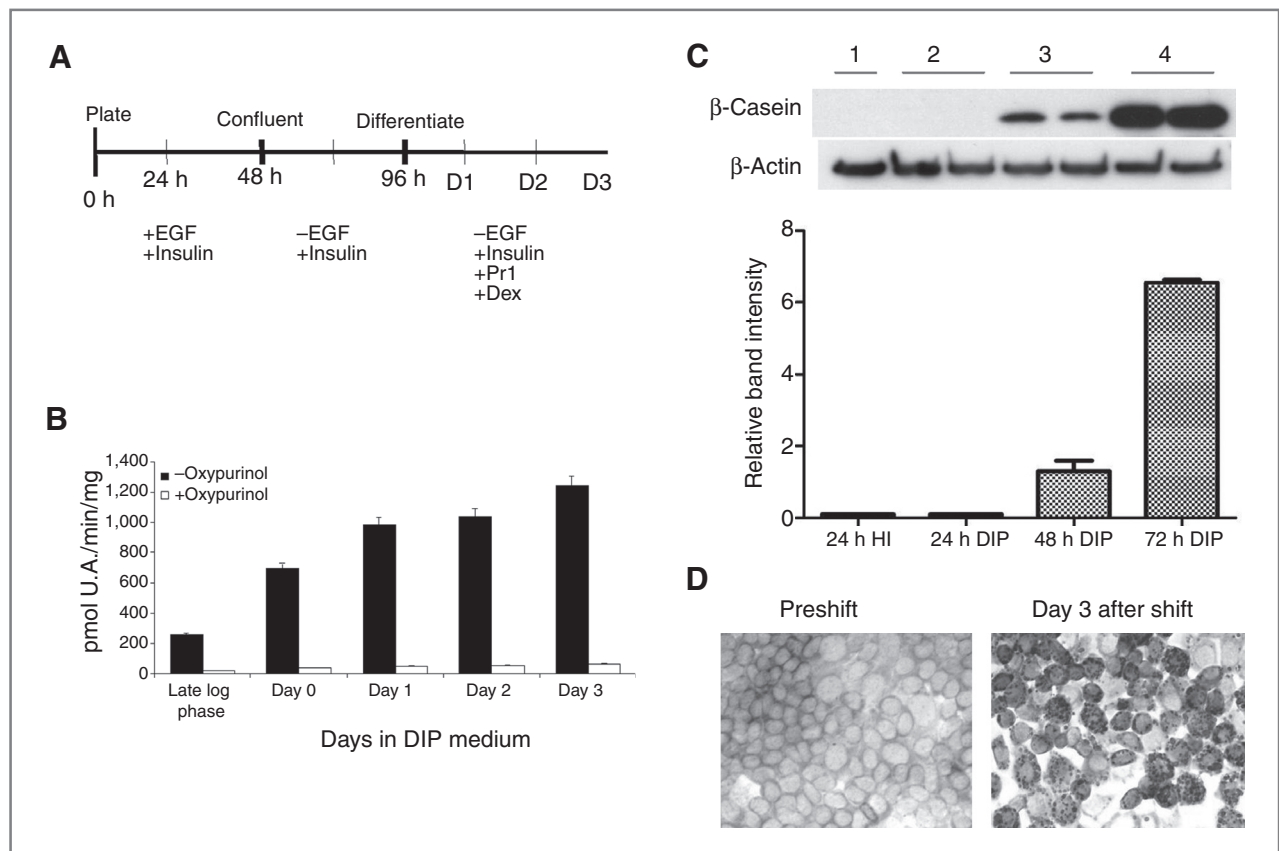


Figure 2. Expression of XOR activity during *in vitro* differentiation of HC11 cells. A, differentiation time course: HC11 cells were grown to confluency in standard growth medium consisting of RPMI 1640, 10% FBS, insulin 5 μ g/mL, EGF 10 ng/mL, and 1 \times GIBCO antibiotic/antimycotic solution. After 48 hours, confluent cells were shifted into serum-free medium without EGF but with insulin. After a further 48 hours, cells were shifted into DIP medium consisting of RPMI 1640, 5 μ g/mL insulin, 10 μ g/mL prolactin (PrI), 10⁻⁷ mol/L dexamethasone (Dex), and 1 \times antibiotic/antimycotic solution. B, XOR activity during HC11 differentiation. Cells were harvested in log phase while in rich growth medium, at day 0 when cells were first shifted into starvation medium, and at days 1, 2, and 3 following the shift into DIP medium. Cell lysates were prepared and total XOR activity was determined by spectroscopic assay of uric acid formation (13). Data are picomoles of uric acid per minute per milligram of protein. The mean \pm SD of 6 determinations (black bars) are shown. Oxypurinol was included in separate reactions at 150 μ mol/L to confirm specificity (open bars) of uric acid generation. C, β -casein was analyzed by Western immunoblotting (top) using the same cell lysates as in B. Band intensity was quantitated by scanning dosimetry, and data show the mean \pm SD of 6 determinations at each time point (bottom). D, Oil Red O staining in differentiated and undifferentiated HC11 cells. Cells were stained by Oil Red O at day 0 before the shift into DIP medium and after 3 days of differentiation in DIP medium.

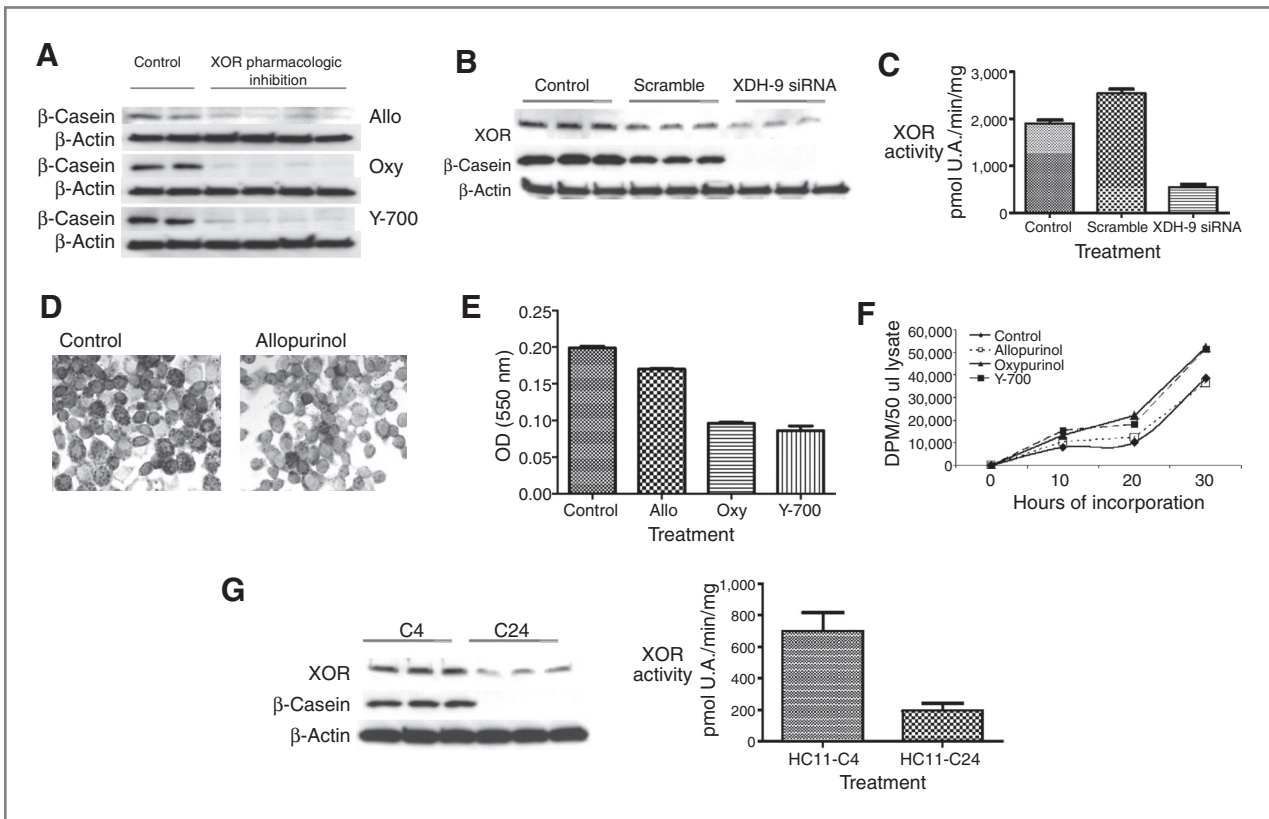


Figure 3. XOR activity is required for *in vitro* differentiation of HC11 cells. A, pharmacologic inhibition of XOR blocked expression of β -casein in differentiating HC11 cells. HC11 cells were grown and differentiated as described in Figure 1. At the end of starvation, cells were shifted into DIP medium in the presence of the XOR inhibitors allopurinol (Allo; 150 μ M/L), oxypurinol (Oxy; 150 μ M/L), or Y-700 (1 μ M/L). Control cells were shifted into DIP without inhibitor. At day 3 following the shift, cells were harvested, lysates prepared, and Western blots conducted against β -casein or β -actin (loading control). Replicate samples from 4 separate experiments are shown. B, anti-XOR-siRNA inhibited expression of β -casein in differentiating HC11 cells. HC11 cells were differentiated as in A and transfected with anti-XOR-siRNA just prior to the shift into DIP medium. Western blots were run against XOR, and β -casein from cells was harvested on day 3 following the shift into DIP medium. C, XOR activity was reduced in parallel with XOR protein by transfection of anti-XOR-siRNA. XOR activity was determined from the same lysates as in B. D, XOR inhibition blocked lipid vesicle development in differentiating HC11 cells. HC11 cells were differentiated as in A and representative samples stained with Oil Red O at day 3 following the shift into DIP medium. E, quantification of Oil Red O staining, which was achieved at day 3 following the shift into DIP medium in the presence or absence of XOR inhibitors. Data show the mean \pm SD of 4 independent replicates. F, pharmacologic inhibition of XOR reduces HC11 proliferation rate. HC11 cells were plated in the presence or absence of XOR inhibitors as shown and incorporation of 3 H-thymidine was measured over the course of the subsequent 30 hours. For oxypurinol and Y-700 versus control, $P < 0.05$ by ANOVA; for allopurinol versus control, P was not significant. G, low XOR-expressing derivatives of HC11 cells fail to induce β -casein during *in vitro* differentiation. Clonally selected derivatives of HC11 cells, C4 and C24, were differentiated as in Figure 1, and Western blots were run against XOR and β -casein from cells harvested at day 3 following the shift into DIP medium (left). XOR activity was measured in C4 and C24 cells differentiated as in A, 3 days after the shift into DIP medium. Data show the mean \pm SD of 3 independent replicates used for Western blot (right).

against XOR or with a scrambled siRNA showing no homology to XOR. We observed strong inhibition of β -casein induction by the anti-XOR-siRNA but not with the scrambled siRNA control (Fig. 3B). Anti-XOR-siRNA, but not the scrambled siRNA control, markedly reduced XOR activity at day 3 following the shift into DIP medium (Fig. 3C). Inhibition of XOR using the same 3 pharmacologic inhibitors also markedly depressed accumulation of vesicle neutral lipid (Fig. 3D and E). Again, and in keeping with the effect observed on β -casein, Allopurinol exerted a less pronounced effect on vesicle neutral lipid accumulation than did oxypurinol or Y-700. Consistent with the role played by XOR in promoting HC11 differentiation, we observed that pharmacologic inhibition of XOR increased growth rate of the cells. Although, again, oxypurinol and

Y-700 exerted a more pronounced effect on growth rate than did allopurinol (Fig. 3F).

HC11-C24 cells failed to induce β -casein during *in vitro* differentiation

We previously characterized clonally selected derivatives of HC11 cells that express XOR (HC11-C4) or express extremely low levels of XOR (HC11-C24; ref. 5). We differentiated HC11-C4 and HC11-C24 cells *in vitro*, and 3 days following the shift into DIP medium, we observed both poor expression of XOR protein level and activity in HC11-C24 cells compared with HC11-C4 cells. HC11-C24 cells, but not HC11-C4 cells, also failed to induce β -casein at day 3 after the shift into DIP medium (Fig. 3G).

Microarray analysis reveals the predictive effect of XOR on both human mammary tumor estrogen receptor status and time to tumor relapse

The impact of XOR expression on human breast cancer was characterized using mRNA microarray analysis. Data were mined from the lymph node-negative breast cancer patients in the Wang mRNA microarray data set (28). Covariance of XOR expression and estrogen receptor (ER) status was conducted by the Spearman rank correlation test. These data employed a binary score for both ER (+ or -) and XOR (High or Low). This produced a set of 286 valid cases (wherein data were generated in this binary fashion), with a correlation coefficient of 0.148529 and a 1-sided P value significance of 0.005954. This is a very strong correlation showing that high XOR mRNA expression was associated with ER⁻ status and that low XOR mRNA expression was associated with ER⁺ status in this data set. Further data mining of the Wang data set for XOR expression and time to tumor relapse showed that XOR varied inversely with time to relapse with $P = 0.03$ level of

significance (Fig. 4A). These data show that high XOR score predicted a delayed time to relapse.

Pharmacologic inhibition of XOR increased tumor growth in a mouse xenograft model of human breast cancer

The contribution of XOR to mammary gland and HC11 differentiation suggested that XOR might modulate tumor cell growth, and very poor expression of XOR was observed in the most aggressive human breast cancer (1). We observed that XOR was also undetected in aggressive tumors from an ErbB2 transgenic mouse model of breast cancer (30); immunofluorescence analysis of these aggressive tumors exhibited nearly undetectable levels of XOR (Fig. 4B). We used a xenograft model of MDA-MB-231 cells in *nu/nu* mice to determine the effect of XOR pharmacologic inhibition on tumor growth. When mice carrying MDA-MB-231 tumors were treated with 3 different inhibitors of XOR over a period of 12 weeks, we observed a statistically significant increase in tumor growth and final

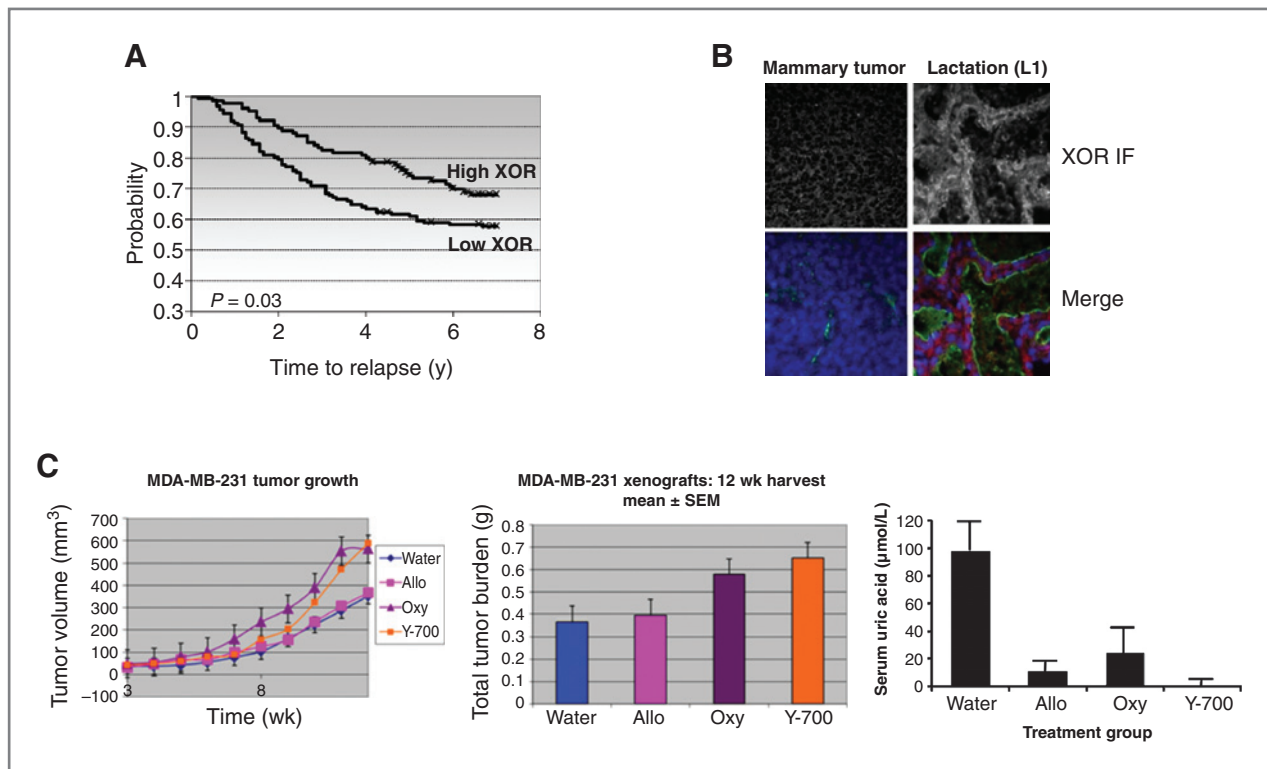


Figure 4. A, data were mined from the Wang RNA microarray data set, which comprises 286 lymph node-negative breast cancer patients (28). XOR correlated inversely with time to relapse with $P = 0.03$ level of significance. In the figure shown, Kaplan-Meier analysis of time to relapse is illustrated for high and low XOR expression. These data show that high XOR score predicts a delayed time to relapse. B, expression of XOR protein in mouse mammary tumors and during lactation *in vivo*. XOR immunofluorescence (IF) and tissue architecture were stained in whole mammary gland tissue as described in Figure 2. Tissues were stained at day 7 of pregnancy and at day 1 of lactation. A mouse mammary adenocarcinoma was also stained for XOR and tissue architecture. C, xenograft tumors of MDA-MB-231 cells were grown in *nu/nu* Nude mice as described in Materials and Methods. Shown are the tumor volumes calculated from caliper measurements over the 12-week time course (left) and the final tumor weight at harvest for the 4 treatment groups: water control, allopurinol (Allo), oxypurinol (Oxy), and Y-700 (middle); significance of difference between each individual inhibitor group and the water control was determined by ANOVA. Allopurinol, P , not significant; oxypurinol, $P < 0.05$; Y-700, $P < 0.05$. Right, serum uric acid was measured at the time of harvest to verify the effect of XOR inhibition. Data show the mean \pm SEM, with 6 mice in each group. Significance of difference between each individual inhibitor group and the water control was determined by 1-sided Student's t test. Allopurinol, $P < 0.02$; oxypurinol, $P < 0.05$; Y-700, $P < 0.001$.

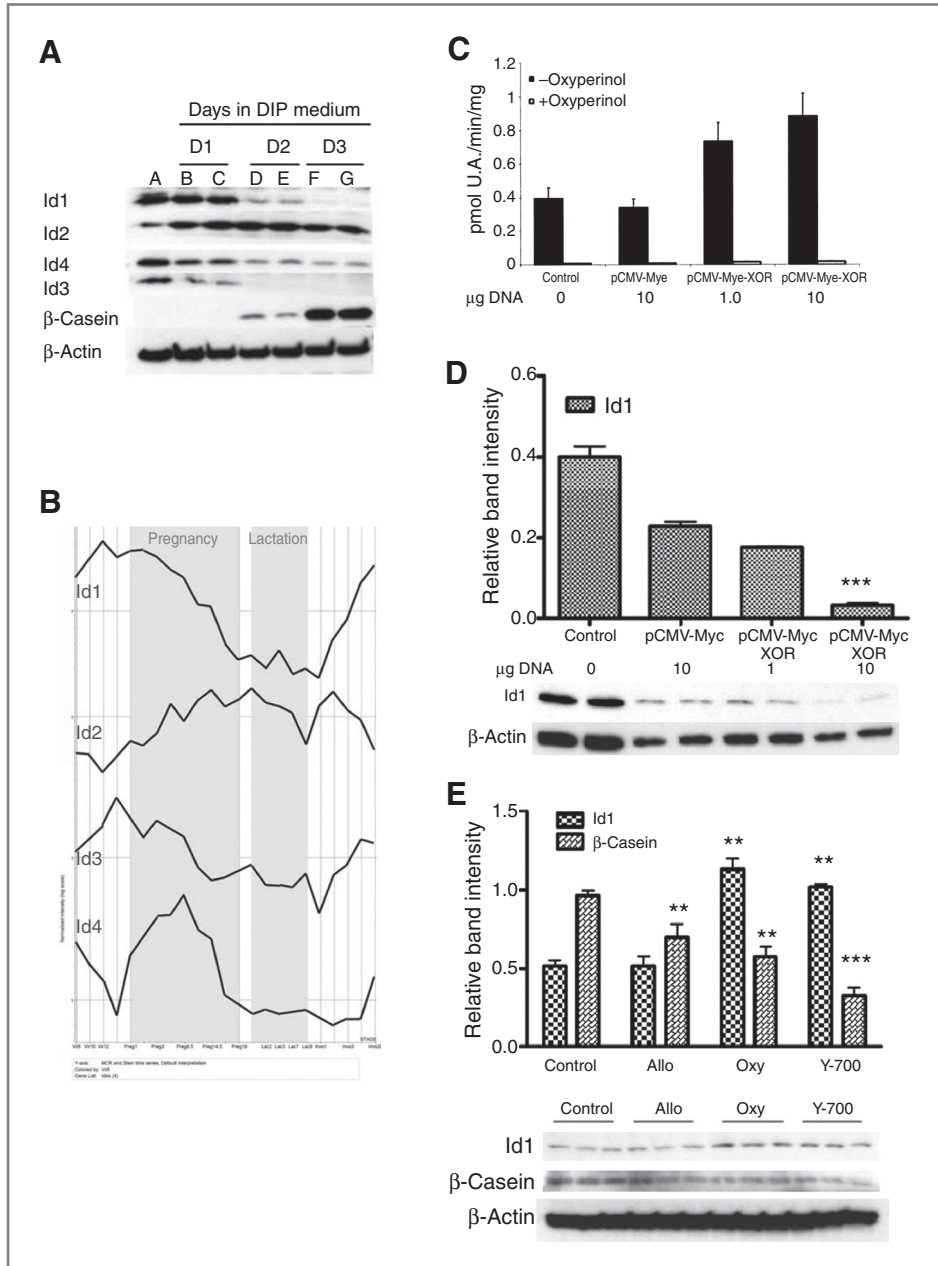


Figure 5. Divergent expression of Id proteins during HC11 differentiation *in vitro* and during mammary gland development *in vivo*. **A**, differential expression of Id proteins in HC11 cells at different stages of differentiation. HC11 cells were differentiated as described in Figure 1. Western blots were run on cell lysates taken at the point of shift into DIP medium and subsequently at days 1, 2, and 3 following the shift. Blots were analyzed with antisera against Id1, Id2, Id3, Id4, and β -casein. Experiments were run in quadruplicate, and duplicate lanes are shown for each day after the shift. **B**, mRNA microarray expression profile of Id proteins 1 to 4 during mouse mammary gland development *in vivo*. Shown is the normalized expression of each Id mRNA over the entire developmental time course: virgin weeks, 6, 10, and 12; pregnancy days, 1, 3, 8.5, 14.5, 17, and 19; lactation days, 1, 2, 3, 7, and 9; and forced-weaning involution days, 1, 2, 3, 4, and 20. **C**, ectopic overexpression of XOR increases XOR activity in undifferentiated HC11 cells. HC11 cells were grown to mid log phase in rich growth medium and were transfected with the pCMV-Myc vector or with pCMV-Myc-XOR at 1.0 and 10.0 μ g per well. XOR activity was determined from 4 replicates, and oxyperinol was used for confirmation. **D**, ectopic overexpression of XOR blocks expression of Id1 in undifferentiated HC11 cells. HC11 cells were grown to mid log phase in rich growth medium and were transfected with the pCMV-Myc vector or with pCMV-Myc-XOR at 1.0 and 10.0 μ g per well. Cells were harvested after 48 hours and Western blots were run against Id1. Replicate blots were scanned, and data for Id1 were normalized to the band intensity of β -actin. Data show the mean \pm SEM, where ***, $P < 0.001$ when the indicated band was compared with control by Student's *t* test. **E**, pharmacologic inhibition of XOR increases Id1 protein level in differentiated HC11 cells. HC11 cells were differentiated as in Figure 1, with inhibitors of XOR added at the point of shift into DIP medium. Western blots were run against Id1 and β -casein at day 3 following the shift into DIP medium. Blots were scanned, quantitated, and normalized as described previously. Data show mean \pm SEM of 3 replicates. **, $P < 0.05$ and ***, $P < 0.001$ when the indicated bands were compared with control by Student's *t* test. Allo, allopurinol; Oxy, oxyperinol.

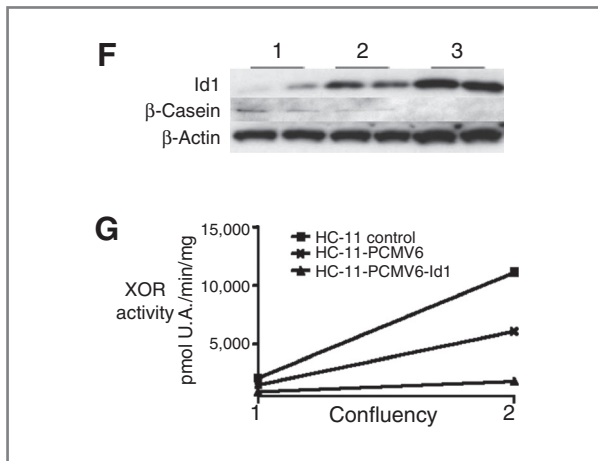


Figure 5. (Continued) F, stable overexpression of Id1 cDNA inhibits β -casein expression in differentiating HC11 cells. HC11 (lane 1), HC11-pCMV6 (lane 2), and HC11-pCMV6-Id1 (lane 3) cell lines were differentiated as described in Figure 1. Cell lysates were prepared at day 3 following the shift into DIP medium, and Western blots were run against Id1 and β -casein. G, XOR activity was determined from the same cell lysates as in E at 3 days following the shift into DIP medium (2) and from cells harvested immediately before the shift (1).

tumor volume in the presence of oxypurinol or Y-700 (Fig. 4C). Although allopurinol treatment produced a similar increase in tumor growth, its effect was significantly smaller than that observed with the other inhibitors. The effectiveness of systemic XOR inhibition was verified by the effect of XOR inhibitors on serum uric acid, which was most profoundly reduced by Y-700 (Fig. 4C).

Id proteins exhibited divergent expression during both HC11 differentiation and mouse mammary gland development

The Id proteins are members of the helix-loop-helix family of transcription factors that exert essential but still poorly understood roles in mammary gland development and breast cancer (31–33). Four Id proteins are presently recognized: Id1, Id2, Id3, and Id4. We examined expression of Id proteins during differentiation of HC11 cells and observed a markedly divergent pattern of expression between the different proteins (Fig. 5A). Id1 protein levels declined precipitously at days 1, 2, and 3 following the shift into DIP medium, whereas Id2 protein levels increased immediately and remained high at days 1, 2, and 3. Id3 and Id4 protein levels declined in parallel with Id1, although the decline in Id4 protein level was not as marked as those for Id1 and Id3.

Microarray analysis of Id mRNA levels throughout the course of mouse mammary gland development revealed equally complex and divergent expression (Fig. 5B). Before the onset of pregnancy, both Id1 and Id3 mRNA levels increased briefly, whereas mRNA levels for Id2 and Id4 decreased. Both Id1 and Id3 mRNA levels declined continuously throughout pregnancy and lactation, whereas mRNA levels for Id2 increased during the same period. Id4 mRNA levels, on the other hand, exhibited dramatic

increase during pregnancy that declined precipitously from mid-pregnancy and throughout lactation. Shortly after the start of involution, Id1 and Id3 mRNA levels increased continuously whereas Id2 mRNA levels declined throughout most of lactation. Id4 mRNA levels showed only an increase during the last few days of involution. The divergent pattern of expression of the different Id mRNAs is consistent with the diverse roles ascribed to Id proteins during mammary gland development and reaffirm that the Id proteins may have distinct and independent functions in development (33).

XOR and Id1 exerted opposite effects on their respective expression

To determine whether HC11 cells with either an empty expression vector (pCMV-Myc) or the XOR expression vector (pCMV-Myc-XOR). These cells showed an expected DNA dose-dependent and oxypurinol-inhibitable increase in XOR activity (Fig. 5C) and the concomitant reduction in levels of Id1 protein on Western immunoblotting (Fig. 5D). Conversely, when HC11 cells were differentiated in the absence or presence of XOR pharmacologic inhibitors, we observed that cells exposed to oxypurinol or Y-700 expressed higher levels of Id1 protein. As described earlier, this was accompanied by parallel decline in β -casein levels (Fig. 5E).

To determine whether ectopic overexpression of Id1 would modulate HC11 differentiation, we developed new stably transfected derivatives of the HC11 cell line that express either the empty expression vector (pCMV6) or overexpress Id1 cDNA in the same vector (pCMV6-Id1). These cells were differentiated *in vitro* and at day 3 following the shift into DIP medium cells were harvested and analyzed. As expected, we observed marked increase in Id1 protein in cells transfected with pCMV6-Id1 (Fig. 5F). The increase in Id1 protein produced with pCMV6-Id1 was accompanied by marked decreases in expression of both β -casein protein levels and XOR activity (Fig. 5F and G). Thus, ectopic overexpression of Id1 mRNA inhibited functional differentiation of HC11 cells by lactogenic hormones.

Ectopic overexpression of XOR augmented HRG β 1-induced differentiation of human mammary cancer cells *in vitro*

It has been shown that HRG β 1 can induce expression of markers of epithelial cell differentiation in various breast cancer cell lines (34). Although XOR was activated in MCF-7 cells that were treated with HRG β 1 (Fig. 6A), we observed only modest inhibition of MCF-7 proliferation by HRG β 1 alone (not shown). However, proliferation was significantly reduced in MCF-7 cells that were stably transfected with pCMV-Myc-XOR to generate high-level constitutive overexpression of XOR (Fig. 6B). The reduction in proliferation was associated with the induction of differentiation measured by the level of HRG β 1-induced production of neutral lipid droplets (ref. 34; Fig. 6B). The

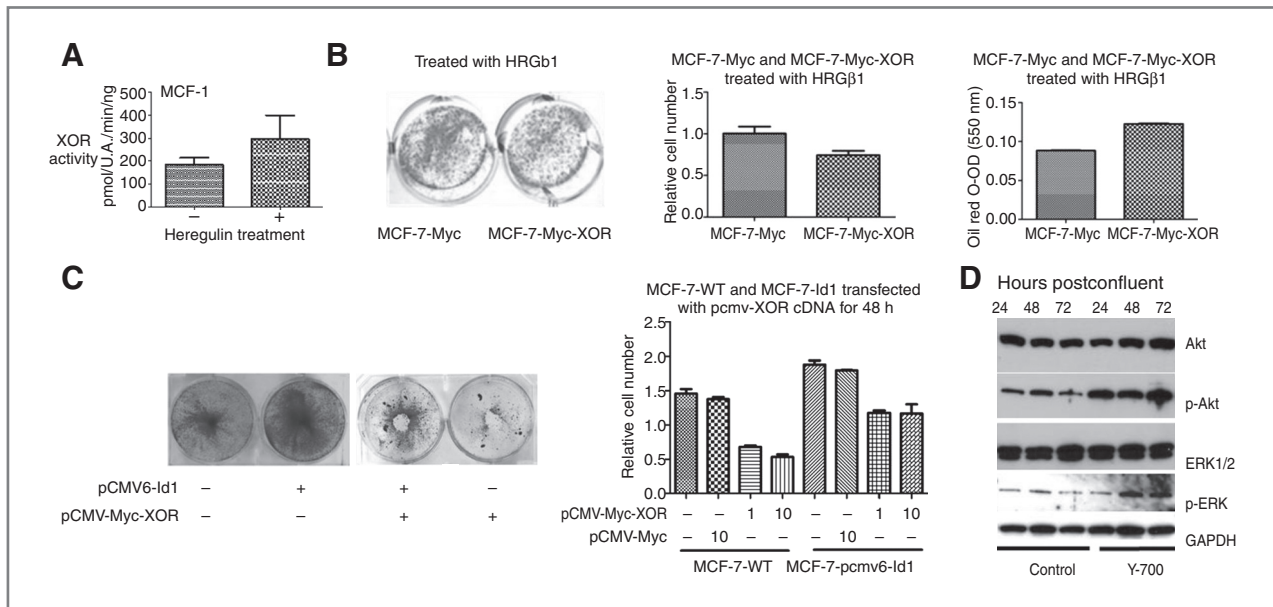


Figure 6. XOR modulates proliferation of human mammary carcinoma cells and tumors. A, XOR activity was increased in human mammary cancer cells by treatment with HRG β 1 (10 ng/mL). XOR activity was measured in MCF-7 human mammary cancer cells 72 hours after treatment with HRG β 1 and in untreated control cells. Data show the mean \pm SEM of 6 independent replicates; $P < 0.05$ by Student's t test. B, MCF-7-Myc and MCF-7-Myc-XOR cells were grown as described previously, treated with HRG β 1, and stained with the SRB. Plates were photographed, and results of 6 independent assays were quantitated. Data show the mean \pm SEM and differed significantly by Student's t test with $P < 0.02$. MCF-7-Myc and MCF-7-Myc-XOR cells were differentiated with HRG β 1, and 72 hours later, cells were stained for neutral lipid with Oil Red O, which was quantitated spectrophotometrically. Data show the mean \pm SEM of 6 independent assays. C, ectopic overexpression of XOR in MCF-7-pCMV6-Id1 cells reduces cell proliferation. MCF-7 wild type (wt) and MCF-7-pCMV6-Id1 cells were grown to late log phase and then transfected with pCMV-Myc-XOR at different levels DNA input. Plates were stained with SRB to identify living cells 72 hours after transfection and were photographed. Results of 4 independent transfections over the DNA concentration range indicated were quantitated to reflect the relative cell number. Data show the mean \pm SEM; data differed significantly by Student's t test for 1.0 and 10.0 μ g of input pCMV-Myc-XOR between MCF-7-WT and MCF-7-pCMV6-Id1 $P < 0.02$ (1.0 μ g DNA) and $P < 0.01$ (10.0 μ g DNA). D, MCF-7 cells were grown 72 hours after reaching confluency in the absence or presence of the XOR inhibitor Y-700. Western blots were run on whole-cell extracts against Akt, p-Akt, ERK, p-ERK, and GAPDH as a control for loading of the gel. GAPDH, glyceraldehyde-3-phosphate dehydrogenase.

augmentation of HRG β 1-induced differentiation by XOR overexpression may result from the relatively low level of XOR found in native MCF-7 cells (5).

Inhibitory effects of XOR on human breast cancer cell proliferation was attenuated by ectopic overexpression of Id1

We have shown the effects of XOR on normal HC11 and human breast cancer cell differentiation. These observations raised the possibility that induction or ectopic overexpression of XOR could be used to inhibit cancer cell proliferation. We observed that transient transfection of MCF-7 cells with pCMV-Myc-XOR resulted in reduced proliferation (Fig. 6C). To determine the effect of Id1 on XOR-induced reduction of proliferation in these cells, we generated stable cell lines of MCF-7 that expressed either pCMV6-Id1 or the empty pCMV6 vector. We observed that Id1 ectopic overexpression not only increased the proliferation of MCF-7 cells but also attenuated the inhibitory effects of XOR on proliferation (Fig. 6C).

Both extracellular signal-regulated kinase (ERK) and Akt mitogen-activated protein kinase (MAPK) signaling cascades contribute to tumor proliferation, progression, and metastasis (35–38), and their activation regulates

expression of key effector molecules (39, 40) involved in tumorigenesis. We observed that both phospho-ERK (p-ERK) and phospho-Akt (p-Akt) were increased in MCF-7 by pharmacologic inhibition of XOR (Fig. 6D). Thus, XOR activity may comprise an important missing link in the signaling cascade that modulates MAPK activation and mammary tumorigenesis. For example, although little is presently known about the impact of p-ERK on MCF-7 Id1, in esophageal cancer, Id1 promotes tumorigenesis in part by phosphoactivation of Akt (41), and this effect is reflected in Id1-overexpressing MCF-7 cells where Id1 also activates the Akt pathway (42). We imagine that one mechanism by which XOR modulates proliferation and Id1 in MCF-7 mammary carcinoma cells is by downregulating levels of p-Akt and p-ERK, and this may comprise one mechanism by which XOR modulates breast cancer.

Discussion

Clinical observations have suggested the possibility that downregulation of XOR may be functionally linked to breast cancer aggressiveness and recurrence. Conversely, expression of XOR was associated with less aggressive breast

cancer and reduced aggressiveness of breast cancer cells *in vitro* (1, 5).

Our studies identified the contribution of XOR to differentiation that was associated with its capacity to modulate proliferation, and these data fully support both mRNA expression profiling in mammary gland development, the inhibition of XOR activity by estrogen (discussed later), and its expression in ER⁻ breast cancer. In conjunction with previous investigations that showed the activation of XOR by lactogenic hormones (6, 10) and identified its physical role in the formation of the lactating MFG (12, 14), these studies identify XOR as a marker of mammary gland development and differentiation. Furthermore, pharmacologic inhibition of XOR activity was found to reduce expression of both β -casein protein and neutral lipid in differentiating HC11 cells, and these observations were confirmed with the use of anti-XOR-siRNA transfection. In addition, clonally selected derivatives of HC11 cells that poorly express XOR failed to induce β -casein during differentiation. Together these data show for the first time that XOR catalytic activity, as opposed to its physical role in the formation of the MFG, is required for functional differentiation of HC11 cells.

The basic helix-loop-helix (bHLH) family of transcription factors includes the Id proteins, Id1, Id2, Id3, and Id4 that are important mediators of mammary gland development and breast tumorigenesis (33). Although the roles of individual Id proteins are not well understood, current data support a role for Id2 in both the development of lactation (43) and the maintenance of a differentiated and noninvasive phenotype (33, 44). Although the specific role of Id1 in both mammary gland development and in neoplastic transformation is presently unclear (45), the cooperation of Id1 and Id3 in triple-negative breast cancer [ER⁻, progesterone (PR)⁻, Her2⁻] and in the progression and proliferation of lung metastasis has been identified (46). We uncovered highly divergent expression of Id proteins during HC11 differentiation and parallel divergence in mRNA expression during mouse mammary gland development *in vivo*, which are consistent with these observations. For example, increased Id2 expression correlated well with HC11 differentiation and with mouse pregnancy and lactation. Expression of both Id1 and Id3 was consistently opposite that of Id2.

Expression of Id1 and XOR proteins was opposite during HC11 differentiation, and their respective mRNA profiles were opposite as well during mammary gland development in the mouse. These data led us to ask whether XOR was itself involved in the expression of Id1 or whether Id1 was involved in the expression of XOR. Remarkably, we observed that XOR and Id1 exerted opposite effects on their respective expression. Ectopic overexpression of XOR repressed Id1 expression in HC11 cells, whereas pharmacologic inhibition of XOR increased Id1 protein level. Conversely, ectopic overexpression of Id1 inhibited differentiation of HC11 cells blocking the expression of both XOR and β -casein. We hypothesized that the opposing expression of XOR and Id1 may comprise an important

mechanism by which XOR expression could modulate breast cancer aggressiveness.

Dysregulation of both XOR and Id1 in the most aggressive human breast cancer (1, 19) led us to ask whether XOR and Id1 might oppositely effect breast cancer cell proliferation. Id1 levels were found to be very high in the most aggressive metaplastic breast cancer (19), whereas XOR levels were found to be extremely low in the most aggressive human breast cancer (1) or breast cancer cells (5). Furthermore, although Id1 is not expressed in normal luminal epithelial cells (47), XOR is an abundant product of these cells. To determine the effect of XOR and Id1 on breast cancer cell proliferation, we developed new cell lines from the MCF-7 luminal carcinoma cell line that stably overexpressed Id1, the MCF-7-pCMV6-Id1 cells. As anticipated from published reports (48), these cells exhibited marked increase in proliferation compared with wild-type MCF-7. Transient overexpression of XOR using pCMV-Myc-XOR in MCF-7-pCMV6-Id1 cells reversed the increase in cell proliferation and in a DNA dose-dependent fashion. Indeed, even in wild-type MCF-7 cells, transient overexpression of XOR also dose dependently inhibited proliferation. We conclude that in human mammary carcinoma cells, as in HC11 cells, XOR and Id1 exert opposing effects on cell proliferation.

The impact of XOR on human mammary cancer *per se* was determined by microarray data mining of XOR mRNA expression. These analyses uncovered the significant predictive value of low XOR expression for the time to tumor relapse. Low XOR expression predicted a more rapid time to tumor relapse. Furthermore, XOR exhibited very poor expression in xenograft analysis of ErbB2 breast cancer tumors. Published reports of Id1 in human breast cancer revealed high Id1 levels to be associated with highly aggressive metaplastic carcinoma (19), with the reinitiation of triple-negative breast cancer-derived lung metastasis (46), and as a key gene mediating both tumorigenesis and lung metastasis in MDA-MB-231 cell xenograft (18). Although we have found XOR to be poorly expressed in MDA-MB-231 cells, expression could be activated pharmacologically to modulate aggressiveness *in vitro* (5). We hypothesize that the expression of XOR observed in luminal breast cancer cells contributes to the poor expression of Id1 observed in these cells and tumors (19, 45), whereas the poor expression of XOR in both the most aggressive human breast cancer and tumors cells (1, 5) removes this restraint on Id1 expression.

Although the previously published clinical analysis of XOR did not show an association with ER status *per se* (1), microarray data mining the Wang data set (28) did reveal a significant association of low XOR expression and ER⁺ status. Furthermore, estrogen stimulated both proliferation and expression of Id1 (48) in ER⁺ T47D human breast cancer cells, whereas estrogen downregulated XOR in both ER⁺ and ER⁻ breast cancer cells (49, 50). Thus, XOR modulation by estrogen seems to be ER independent and modulation of XOR by estrogen may comprise part of the mechanism by which reduced XOR expression contributes

to breast cancer aggressiveness. Differences in the data sets used to correlate XOR expression with ER status (Finnish versus North America, breast cancer subtype classification, age, and race composition) may be responsible for the different results obtained in these 2 studies.

Results presented here, in conjunction with published reports showing the effects of low XOR expression on tumor cell aggressiveness *in vitro* (5) and on mammary tumor aggressiveness *in vivo* (1), identify XOR as an important functional component of differentiation and proliferation whose diminished expression contributes to breast cancer aggressiveness. Recent publications identified a group of signature genes, which comprise in part *Id1*, *COX-2*, and *MMP-1*, that mediate breast cancer metastasis to the lung (18, 46), and of these, *Id1* was found to be a signature gene for tumorigenesis as well (18). Remarkably, XOR has now been found to modulate expression of *Id1*, *COX-2*, and *MMP-1* (5). Although *Id1* is poorly expressed in some breast cancer (19, 45), its overexpression in the most aggressive metaplastic breast cancer is consistent with the observation that poor XOR expression is associated with the most aggressive human breast cancer. Downregulation of *Id1* has been suggested as a potential therapeutic avenue for aggressive breast cancer (32), and modulation of *Id1* by ectopic overexpression of XOR suggests that pharmacologic

activation of XOR may constitute a novel strategy for the management of the most aggressive and therapeutically resistant breast cancer.

Disclosure of Potential Conflicts of Interest

No potential conflicts of interest were disclosed.

Acknowledgments

The authors thank Dr. Atushi Fukunari (Mitsubishi Tanabe Pharma Corporation) for the XOR inhibitor, Y-700. The authors also thank Dr. Peggy Neville (Department of Physiology, School of Medicine, UCD) for maintaining and providing access to the gene expression data. Paraffin-embedded mammary tissues were the kind gift of Dr. Carol Palmer (UCD Animal Care Committee) and Dr. Jim McManaman (Department of Obstetrics & Gynecology, School of Medicine, UCD).

Grant Support

This work was supported by the generosity of the Robert and Helen Kleberg Foundation, the American Cancer Society (grants: PF-06-005-01-CCE, PF-08-112-01-CCE), and by the NIH (grants: P20-CA103680, T32-HL007171, and RO1-HL045582).

The costs of publication of this article were defrayed in part by the payment of page charges. This article must therefore be hereby marked *advertisement* in accordance with 18 U.S.C. Section 1734 solely to indicate this fact.

Received April 20, 2011; revised June 23, 2011; accepted July 15, 2011; published OnlineFirst July 20, 2011.

References

- Linder N, Lundin J, Isola J, Lundin M, Raivio KO, Joensuu H. Down-regulated xanthine oxidoreductase is a feature of aggressive breast cancer. *Clin Cancer Res* 2005;11:4372–81.
- Cook WS, Chu R, Saksela M, Raivio KO, Yelandi A. V. Differential immunohistochemical localization of xanthine oxidase in normal and neoplastic human breast epithelium. *Int J Oncol* 1997;11:1013–7.
- Lewin I, Lewin R, Bray RC. Xanthine oxidase activity during mammary carcinogenesis in mice. *Nature* 1957;180:763–4.
- Shan L, He M, Yu M, Qiu C, Lee NH, Liu ET, et al. cDNA microarray profiling of rat mammary gland carcinomas induced by 2-amino-1-methyl-6-phenylimidazo[4,5-b]pyridine and 7,12-dimethylbenz[a]anthracene. *Carcinogenesis* 2002;23:1561–8.
- Fini MA, Orchard-Webb D, Kosmider B, Amon JD, Kelland R, Shibao G, et al. Migratory activity of human breast cancer cells is modulated by differential expression of xanthine oxidoreductase. *J Cell Biochem* 2008;105:1008–26.
- McManaman JL, Hanson L, Neville MC, Wright RM. Lactogenic hormones regulate xanthine oxidoreductase and beta-casein levels in mammary epithelial cells by distinct mechanisms. *Arch Biochem Biophys* 2000;373:318–27.
- Linder N, Rapola J, Raivio KO. Cellular expression of xanthine oxidoreductase protein in normal human tissues. *Lab Invest* 1999;79:967–74.
- Garattini E, Mendel R, Romao MJ, Wright R, Terao M. Mammalian molybdo-flavoenzymes, an expanding family of proteins: structure, genetics, regulation, function and pathophysiology. *Biochem J* 2003;372:15–32.
- Anderson SM, Rudolph MC, McManaman JL, Neville MC. Key stages in mammary gland development. Secretory activation in the mammary gland: it's not just about milk protein synthesis! *Breast Cancer Res* 2007;9:204.
- Kurosaki M, Zanotta S, Li Calzi M, Garattini E, Terao M. Expression of xanthine oxidoreductase in mouse mammary epithelium during pregnancy and lactation: regulation of gene expression by glucocorticoids and prolactin. *Biochem J* 1996;319:801–10.
- McManaman JL, Neville MC, Wright RM. Mouse mammary gland xanthine oxidoreductase: purification, characterization, and regulation. *Arch Biochem Biophys* 1999;371:308–16.
- McManaman JL, Palmer CA, Wright RM, Neville MC. Functional regulation of xanthine oxidoreductase expression and localization in the mouse mammary gland: evidence of a role in lipid secretion. *J Physiol* 2002;545:567–79.
- Seymour KJ, Roberts LE, Fini MA, Parnley LA, Oustitch TL, Wright RM. Stress activation of mammary epithelial cell xanthine oxidoreductase is mediated by p38 MAPK and CCAAT/enhancer-binding protein-beta. *J Biol Chem* 2006;281:8545–58.
- Vorbach C, Scriven A, Capecchi MR. The housekeeping gene xanthine oxidoreductase is necessary for milk fat droplet enveloping and secretion: gene sharing in the lactating mammary gland. *Genes Dev* 2002;16:3223–35.
- Singh B, Berry JA, Shoher A, Ramakrishnan V, Lucci A. COX-2 overexpression increases motility and invasion of breast cancer cells. *Int J Oncol* 2005;26:1393–9.
- Ohtsubo T, Rovira II, Starost MF, Liu C, Finkel T. Xanthine oxidoreductase is an endogenous regulator of cyclooxygenase-2. *Circ Res* 2004;95:1118–24.
- Shin MH, Moon YJ, Seo JE, Lee Y, Kim KH, Chung JH. Reactive oxygen species produced by NADPH oxidase, xanthine oxidase, and mitochondrial electron transport system mediate heat shock-induced MMP-1 and MMP-9 expression. *Free Radic Biol Med* 2008;44:635–45.
- Minn AJ, Gupta GP, Siegel PM, Bos PD, Shu W, Giri DD, et al. Genes that mediate breast cancer metastasis to lung. *Nature* 2005;436:518–24.
- Perk J, Gil-Bazo I, Chin Y, de Candia P, Chen JJ, Zhao Y, et al. Reassessment of *id1* protein expression in human mammary, prostate, and bladder cancers using a monospecific rabbit monoclonal anti-*id1* antibody. *Cancer Res* 2006;66:10870–7.
- Terao M, Cazzaniga G, Ghezzi P, Bianchi M, Falciani F, Perani P, et al. Molecular cloning of a cDNA coding for mouse liver xanthine

- dehydrogenase. Regulation of its transcript by interferons *in vivo*. *Biochem J* 1992;283:863–70.
21. Noren NK, Foos G, Hauser CA, Pasquale EB. The EphB4 receptor suppresses breast cancer cell tumorigenicity through an Abl-Crk pathway. *Nat Cell Biol* 2006;8:815–25.
 22. Matsuda Y, Schlange T, Oakeley EJ, Boulay A, Hynes NE. WNT signaling enhances breast cancer cell motility and blockade of the WNT pathway by sFRP1 suppresses MDA-MB-231 xenograft growth. *Breast Cancer Res* 2009;11:R32.
 23. Tanaka T, Doi K, Maeda-Mamiya R, Negishi K, Portilla D, Sugaya T, et al. Urinary L-type fatty acid-binding protein can reflect renal tubulointerstitial injury. *Am J Pathol* 2009;174:1203–11.
 24. Wu X, Wakamiya M, Vaishnav S, Geske R, Montgomery C Jr, Jones P, et al. Hyperuricemia and urate nephropathy in urate oxidase-deficient mice. *Proc Natl Acad Sci U S A* 1994;91:742–6.
 25. Tomayko MM, Reynolds CP. Determination of subcutaneous tumor size in athymic (nude) mice. *Cancer Chemother Pharmacol* 1989;24:148–54.
 26. Stein T, Morris JS, Davies CR, Weber-Hall SJ, Duffy MA, Heath VJ, et al. Involution of the mouse mammary gland is associated with an immune cascade and an acute-phase response, involving LBP, CD14 and STAT3. *Breast Cancer Res* 2004;6:R75–91.
 27. Rudolph MC, McManaman JL, Hunter L, Phang T, Neville MC. Functional development of the mammary gland: use of expression profiling and trajectory clustering to reveal changes in gene expression during pregnancy, lactation, and involution. *J Mammary Gland Biol Neoplasia* 2003;8:287–307.
 28. Wang Y, Klijn JG, Zhang Y, Sieuwerts AM, Look MP, Yang F, et al. Gene-expression profiles to predict distant metastasis of lymph-node-negative primary breast cancer. *Lancet* 2005;365:671–9.
 29. Hynes NE, Taverna D, Harwerth IM, Ciardiello F, Salomon DS, Yamamoto T, et al. Epidermal growth factor receptor, but not c-erbB-2, activation prevents lactogenic hormone induction of the beta-casein gene in mouse mammary epithelial cells. *Mol Cell Biol* 1990;10:4027–34.
 30. Kim A, Liu B, Ordonez-Ercan D, Alvarez KM, Jones LD, McKimmey C, et al. Functional interaction between mouse erbB3 and wild-type rat c-neu in transgenic mouse mammary tumor cells. *Breast Cancer Res* 2005;7:R708–18.
 31. Ling MT, Wang X, Zhang X, Wong YC. The multiple roles of Id-1 in cancer progression. *Differentiation* 2006;74:481–7.
 32. Fong S, Debs RJ, Desprez PY. Id genes and proteins as promising targets in cancer therapy. *Trends Mol Med* 2004;10:387–92.
 33. Desprez PY, Sumida T, Coppe JP. Helix-loop-helix proteins in mammary gland development and breast cancer. *J Mammary Gland Biol Neoplasia* 2003;8:225–39.
 34. Sellappan S, Grijalva R, Zhou X, Yang W, Eli MB, Mills GB, et al. Lineage infidelity of MDA-MB-435 cells: expression of melanocyte proteins in a breast cancer cell line. *Cancer Res* 2004;64:3479–85.
 35. Whyte J, Bergin O, Bianchi A, McNally S, Martin F. Key signalling nodes in mammary gland development and cancer. Mitogen-activated protein kinase signalling in experimental models of breast cancer progression and in mammary gland development. *Breast Cancer Res* 2009;11:209.
 36. Myers AP, Cantley LC. Targeting a common collaborator in cancer development. *Sci Transl Med* 2010;2:48ps45.
 37. Yang W, Ju JH, Lee KM, Shin I. Akt isoform-specific inhibition of MDA-MB-231 cell proliferation. *Cell Signal* 2011;23:19–26.
 38. Mester J, Redeuilh G. Proliferation of breast cancer cells: regulation, mediators, targets for therapy. *Anticancer Agents Med Chem* 2008;8:872–85.
 39. Dhillon AS, Hagan S, Rath O, Kolch W. MAP kinase signalling pathways in cancer. *Oncogene* 2007;26:3279–90.
 40. Andersen JN, Sathyanarayanan S, Di Bacco A, Chi A, Zhang T, Chen AH, et al. Pathway-based identification of biomarkers for targeted therapeutics: personalized oncology with PI3K pathway inhibitors. *Sci Transl Med* 2010;2:43ra55.
 41. Li B, Tsao SW, Li YY, Wang X, Ling MT, Wong YC, et al. Id-1 promotes tumorigenicity and metastasis of human esophageal cancer cells through activation of PI3K/AKT signaling pathway. *Int J Cancer* 2009;125:2576–85.
 42. Lee JY, Kang MB, Jang SH, Qian T, Kim HJ, Kim CH, et al. Id-1 activates Akt-mediated Wnt signaling and p27(Kip1) phosphorylation through PTEN inhibition. *Oncogene* 2009;28:824–31.
 43. Mori S, Nishikawa SI, Yokota Y. Lactation defect in mice lacking the helix-loop-helix inhibitor Id2. *EMBO J* 2000;19:5772–81.
 44. Itahana Y, Singh J, Sumida T, Coppe JP, Parrinello S, Bennington JL, et al. Role of Id-2 in the maintenance of a differentiated and non-invasive phenotype in breast cancer cells. *Cancer Res* 2003;63:7098–105.
 45. Nair R, Junankar S, O'Toole S, Shah J, Borowsky AD, Bishop JM, et al. Redefining the expression and function of the inhibitor of differentiation 1 in mammary gland development. *PLoS One* 2010; 5:e11947.
 46. Gupta GP, Perk J, Acharyya S, de Candia P, Mittal V, Todorova-Manova K, et al. ID genes mediate tumor reinitiation during breast cancer lung metastasis. *Proc Natl Acad Sci U S A* 2007;104:19506–11.
 47. Uehara N, Chou YC, Galvez JJ, de-Candia P, Cardiff RD, Benzra R, et al. Id-1 is not expressed in the luminal epithelial cells of mammary glands. *Breast Cancer Res* 2003;5:R25–9.
 48. Lin CQ, Singh J, Murata K, Itahana Y, Parrinello S, Liang SH, et al. A role for Id-1 in the aggressive phenotype and steroid hormone response of human breast cancer cells. *Cancer Res* 2000;60:1332–40.
 49. Budhiraja R, Kayyali US, Karamsetty M, Fogel M, Hill NS, Chalkley R, et al. Estrogen modulates xanthine dehydrogenase/xanthine oxidase activity by a receptor-independent mechanism. *Antioxid Redox Signal* 2003;5:705–11.
 50. Taibi G, Carruba G, Miceli V, Cocciadiferro L, Nicotra CM. Estradiol decreases xanthine dehydrogenase enzyme activity and protein expression in non-tumorigenic and malignant human mammary epithelial cells. *J Cell Biochem* 2009;108:688–92.